A Compact Monopole Antenna with Reconfigurable Band Notch for Underlay Cognitive Radio Applications

Ali A. Mohammed,
Department of Electrical Engineering
College of Engineering,
University of Basrah,
Basrah, Iraq
a111li@yahoo.com

Falih M. Alnahwi,
Department of Electrical Engineering
College of Engineering,
University of Basrah,
Basrah, Iraq
fmmm1983@yahoo.com

Abdulkareem S. Abdullah
Department of Electrical Engineering
College of Engineering,
University of Basrah,
Basrah, Iraq
kareem134@yahoo.com

Abdul Ghafor A. Abdul Hameed
Department of Electrical Techniques
Qurna Technique Institute,
Southern Technical University,
Basrah, Iraq
abdulgafoorabd@yahoo.com

***Abstract*— A compact printed ultra-wide band (UWB) antenna with a switchable band notch for underlay cognitive radio applications is presented in this paper. The antenna patch is partially covered by a ground plane with a staircase slot in order to enhance the matching between the feed line and the antenna. A broadband notch centered at 3.5 GHz and extended along the frequency range (2.9-3.9) GHz is produced by etching a complementary split-ring resonator on the radiating patch, while the presence and absence of this band notch are controlled by a PIN diode. On the other hand, the sensing mode of the proposed antenna scans a frequency range with a fractional bandwidth equal to 130.6% over the range (2.3-11.16) GHz. The results show that the proposed antenna has reasonable radiation characteristics with omnidirectional radiation pattern suitable for portable devices. The gain value surpasses 2.5 dBi over the entire sensing range, but it drops to value less than -4 dB within the notched band. Furthermore, the fabricated version of the proposed antenna gives measurements that are in good agreement with the simulated results.**

Keywords*— *Ultra-Wideband Antenna, Underlay Cognitive Radio, Band Notch, Split-Ring Resonator, PIN diode.

I. INTRODUCTION

The exponential growth in all forms of wireless telecommunication systems caused a noticeable congestion in the radio frequency (RF) spectrum specified for these applications. Luckily, some of the wireless applications are not used continuously, so they may be idle for a while and their spectrum remains unused from time to time. Cognitive radio (CR) systems have been proposed to utilize the idle spectrum for another unlicensed application (secondary user) as long as the original licensed application (primary user) is inactive. CR applications can be classified to interweave and underlay systems [1]. In interweave CR, the system requires an ultra-wideband (UWB) antenna to sense the presence and the absence of the primary users and another narrow band reconfigurable antenna for communication purposes. However, underlay CR uses the same UWB antenna for both sensing and communication alternately. Since the Federal Communication Commission specifies the frequency range (3.1-10.6) GHz for the UWB applications [2], the communication mode of the underlay CR interferes with some already existing applications that share this range of frequencies such as IEEE 802.16 WiMAX that operate at (3.3–3.7) GHz band, and IEEE 802.11a WLAN, operating at (5.15–5.85) GHz band, and HYPERLAN/2 at (5.425–6.150) GHz. To overcome this issue, reconfigurable band notches should be presented during the communication mode of the UWB antenna to filter out the radiation of the primary application during its active mode [3-6].

In the underlay CR communication systems, the secondary users can access the spectrum-bands of the primary users with a very reduced amount of radiated power spreading over the entire UWB spectrum [7-8] as illustrated in Fig.1 [9]. Unfortunately, some critical applications do not accept any amount of interference, so it is important to avoid the transmission within their bands during their active mode. This can be achieved by presenting a reconfigurable band notch in the communicating UWB antenna. The band notch reconfigurability can be performed with the aid of PIN diodes, varactor diodes, photoconductive switches, micro-electro mechanical (MEMS) switches, and so on. For instance, a pair of PIN diodes was used to control the length of a circular slot etched on the patch of a printed circuit antenna in order to generate two reconfigurable band notches [10]. A varactor diode was embedded on an E-shaped slot to present a tunable band notch covering the frequency range of the 5GHz WLAN applications [11]. A band notch was also reconfigured by mounting a photoconductive switch across a T-shaped slot to eliminate the radiation of the WiMAX applications [12]. Finally, a band notch was generated by modifying the slot length of an elliptical planar monopole antenna owing on the operation of a MEMS switch [13].

This paper proposes a compact printed monopole antenna with a reconfigurable band notch for underlay cognitive radio communication systems. A staircase slot is presented in the ground plane to improve the matching between the feed line and the antenna patch. The band notch is generated by etching a complementary split ring resonator (CSRR) on the antenna

radiating patch to reject the radiation of the WiMAX applications. The reconfigurability of the band notch is accomplished by embedding a PIN diode across the CSRR to provide. The results show superior frequency domain and radiation characteristics over the entire UWB band with very good elimination for the WiMAX radiation, and the measurements are well agreed with the simulated results.

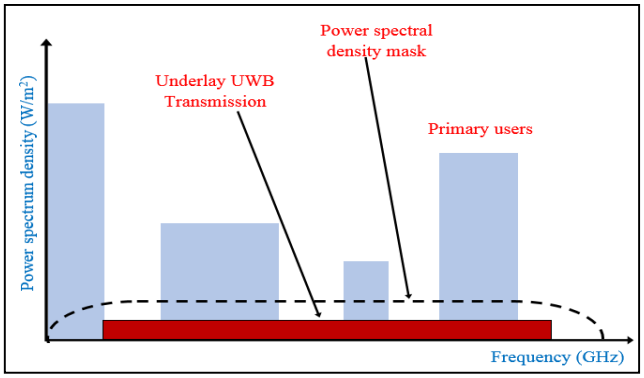

Fig. 1. Underlay cognitive radio (CR) [9]

II. ANTENNA STRUCTURE

Fig. 2 illustrates the front and the back view of the proposed antenna attached to a 50 Ω microstrip feed line. The dielectric substrate of the antenna is an FR4 with dielectric constant ε_r=4.4, loss tangent of 0.025, and height h=1.6mm. The antenna patch includes a trapezoid shaped CSRR responsible for the generation of a band notch to eliminate the WiMAX radiation. A PIN diode is inserted across the CSRR to control the presence and absence of the notched band. A staircase slot is presented in the ground plane to improve the matching between the feed line and the antenna patch, and the bottom side of the patch is also modified for the same purpose. Since the antenna gain and bandwidth are directly affected by the antenna size [14], the size reduction should insure reasonable antenna gain in addition to the antenna bandwidth improvement. This condition has been taken in to account when the antenna size is reduced to (26×32×1.6) mm^3.

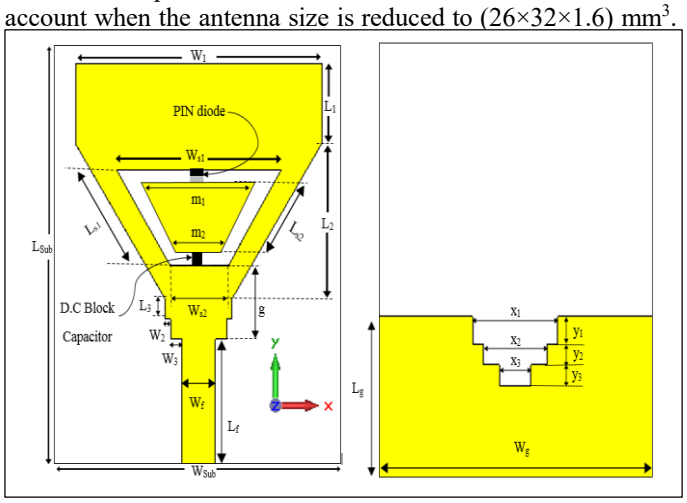

Fig. 2. The proposed antenna configuration Front view (b) Back view

III. PARAMETRIC STUDY

The proposed antenna requires some design steps to reach the intended characteristics. Therefore, the following subsections include a parametric study for the design steps of the antenna and another parametric study about controlling the band notch generated by the proposed CSRR. The parametric study is performed by the Computer Simulation Technology (CST) Microwave studio [15]

A) Antenna Design Steps

Fig. 3 illustrates the design steps of the proposed antenna starting from the ordinary rectangular monopole antenna and ending in the final structure of the antenna with its CSRR. The ordinary structure of the rectangular printed antenna does not achieve the desirable frequency response of the ultra-wideband range. Therefore, the bottom edges of the radiating patch are tapered to enhance the antenna bandwidth as shown in Fig. 3(b). A staircase slot is etched on the ground plane to implement a defective ground structure (DGS) (see Fig. 3 (c)). Since the staircase slot modifies the distance between the bottom edge of the patch and the ground plane, the capacitive coupling between the antenna and the ground plane is modified too resulting in wider impedance bandwidth [16-17]. Another modification at the top end of the feeding line can achieve the desired ultra-wideband response of (2.34–11.16) GHz as illustrated in Fig. 3 (d). In order to obtain a band notch in the frequency response of the proposed antenna, a trapezoid shaped CSRR is engraved on the antenna radiating patch as presented in Fig. 3 (e). The simulated reflection coefficient corresponding to each antenna structure is illustrated in Fig. 4.

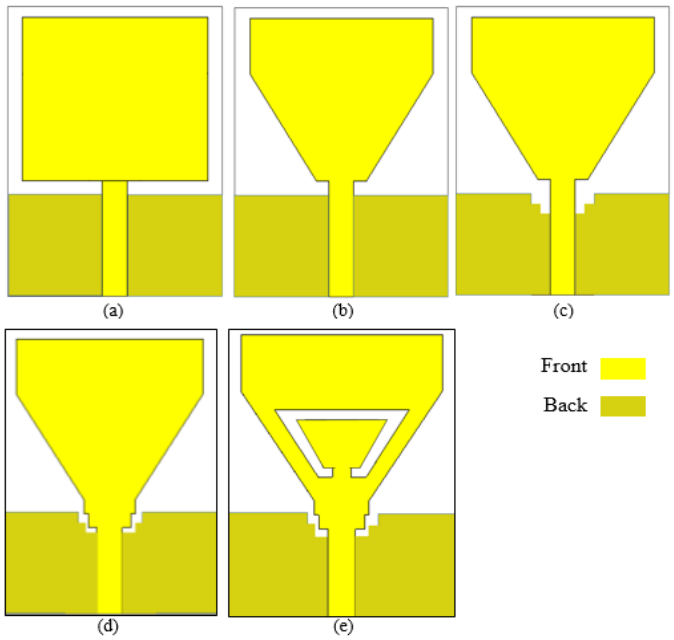

Fig. 3. Different antenna structures that used in simulation studies (a) Basic rectangular antenna with partial ground, (b) Antenna with modified edge of the patch, (c) Antenna with a staircase rectangular slot in the ground plane, (d) Antenna that UWB range achieved, **(e)** Proposed antenna

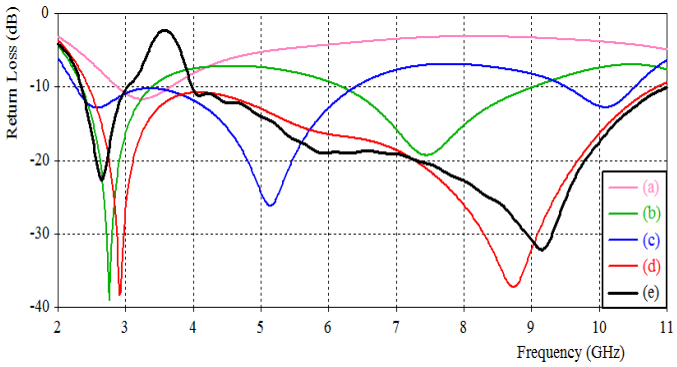

Fig. 4. The simulated reflection coefficient S_{11} of different antenna design steps

B) 3.2 BAND NOTCH GENERATION

As mentioned in Section 1, the antenna should have a reconfigurable band notch to filter out certain application whenever this application is radiating an electromagnetic energy. Therefore, the antenna is operating in two modes depending on the biasing of the PIN diode. The ON state of the PIN diode (forward biasing) can be simulated by a forward resistance R_s in series with a series inductance L_s as shown in Fig. 5(a). On the other hand, the diode OFF state (reverse biasing) can be modeled as a capacitor C_T in parallel with a large value resistor and both are in series with an inductor L_s as exhibited in Fig. 5(b). In this paper a BAP64-02 PIN diode is used with R_s= 2 Ω at 10 mA, C_T = 0.3 pF, and L_s = 0.6 nH [18].

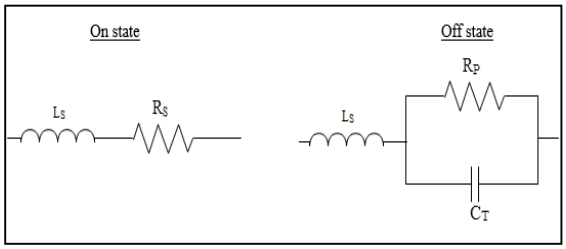

Fig. 5. The equivalent circuit of PIN diode (a) ON state, (b) OFF state

The slot length can determine the center frequency of the band notch. The slot length is approximately equal to half the guided wavelength of the proposed patch antenna ($\lambda_g/2$). As a result, the center frequency of the band notch (f_{notch}) can be predicted using the following formula [19]:

$$f_{notch} = c/2\ell\ (\varepsilon_{re})^{0.5} \quad (1)$$

where (ℓ) represents the total length of the slot, (c) denotes the speed of the light in free space, and (ε_{re}) is the effective dielectric constant of the monopole antenna, which is given by [20-21]:

$$\varepsilon_{re} = (\varepsilon_r+1)/2 \quad (2)$$

Fig. 6(a) and (b) reveals the effect of the slot parts lengths (Ws_1) and (Ls_1), respectively, on the antenna reflection coefficient. However, to verify the minor effect of the staircase matching stub on the band notch, the antenna reflection coefficient for different staircase slot length dimensions is illustrated in Fig. 6(c). It is clear that the dimension of the slot has no influence on the band notch although they control the overall bandwidth of the proposed antenna. TABLE I schedules the best parameters that are obtained by performing the aforementioned parametric study.

TABLE I. Best values of the design parameters [unit: mm]

Wg	**W_1**	**W_2**	**W_3**	**Ws_1**	**Ws_2**	**X_1**	**X_2**
26	22	0.5	0.5	14	4.5	8	6
X_3	**W_f**	**L_{Sub}**	**L_1**	**L_2**	**L_3**	**L_{S1}**	**L_{S2}**
3	3	32	6	11.5	1.5	6.5	5.4
y_1	**y_2**	**y_3**	**L_f**	**L_g**	**m_1**	**m_2**	**g**
2	1.5	1.5	9.5	12	10	3.9	4.5

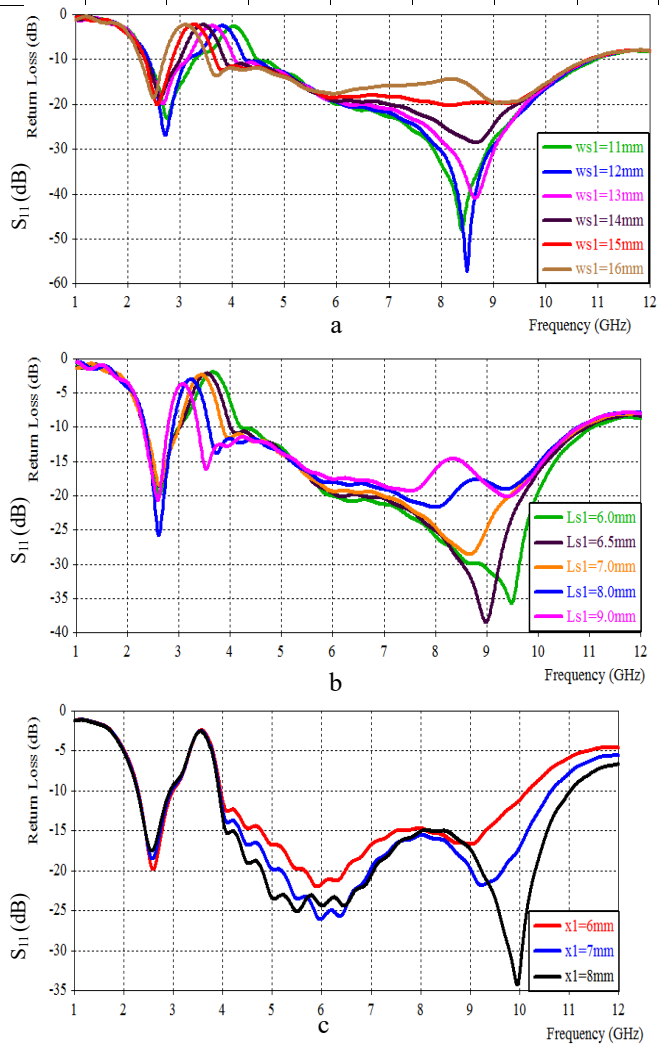

Fig. 6. (a): The simulated reflection coefficient S11 of different values of (ws1) for the trapezoid CSRR slot (b): The simulated reflection coefficient S11 of different values of (Ls1) for the trapezoid CSRR slot(c): The simulated reflection coefficient S11 of different values of (x1) of the staircase ground plane

To understand the band notch generation and the circumstances behind the electronic switching process, the surface current distribution for different switching modes within

and outside the notched band is shown in Fig. 7. For the OFF state of the PIN diode, the current is highly condensed around the slot compared to the other antenna parts. It means that the energy is stored around the band rejection element at frequencies within the notched band. In addition, it can be noted that the current moves in two opposite directions resulting in canceling the electromagnetic radiation under this condition.

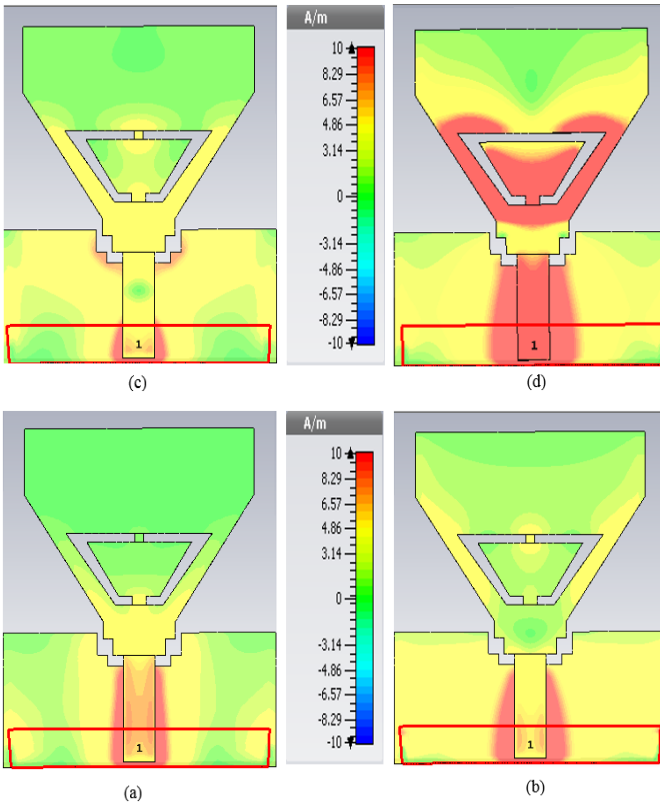

Fig. 7. The current distribution of the proposed antenna when (a) The switch is ON at 2.7GHz,(b) The switch is ON at 3.5GHz, (c) The switch is ON at 6.25GHz, and (d) The switch is OFF at 3.5GHz.

IV. MEASURED RESULTS

Fig. 8 exhibits the front and the back views of the prototype of the proposed antenna. The measurements were taken with the aid of AMITEC network analyzer at University of Basrah/Department of Electrical Engineering. The measured and simulated reflection coefficients of the proposed antenna are illustrated in Fig. 9. It is obvious from Fig. 9(a) that the proposed antenna presents UWB characteristics with a fractional bandwidth of 130.6% (2.34–11.16) GHz for the sensing phase of underlay cognitive radio, whereas Fig. 9(b) reveals the antenna stop band with fractional bandwidth 29.4% (2.9-3.9) GHz for WiMAX interference avoidance. The measured reflection coefficient is congruent with the simulated one for most of the ultra-wideband range. The discrepancy between the simulation and measurements may be attributed to the imperfect soldering of the SMA connector, the unintended coupling of biasing wires of the PIN diodes, or the misalignment of the PIN diode.

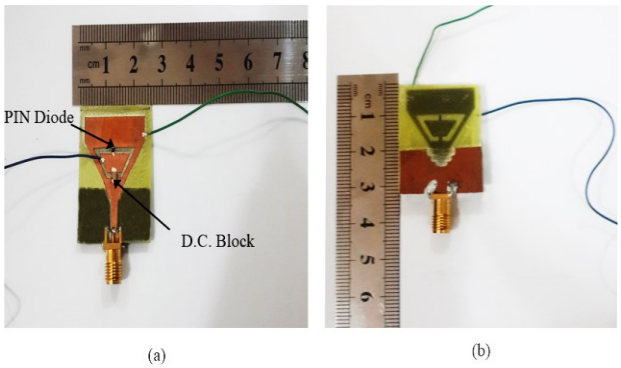

Fig. 8. A photograph of the proposed antenna configuration (a) Front view (b) Back view

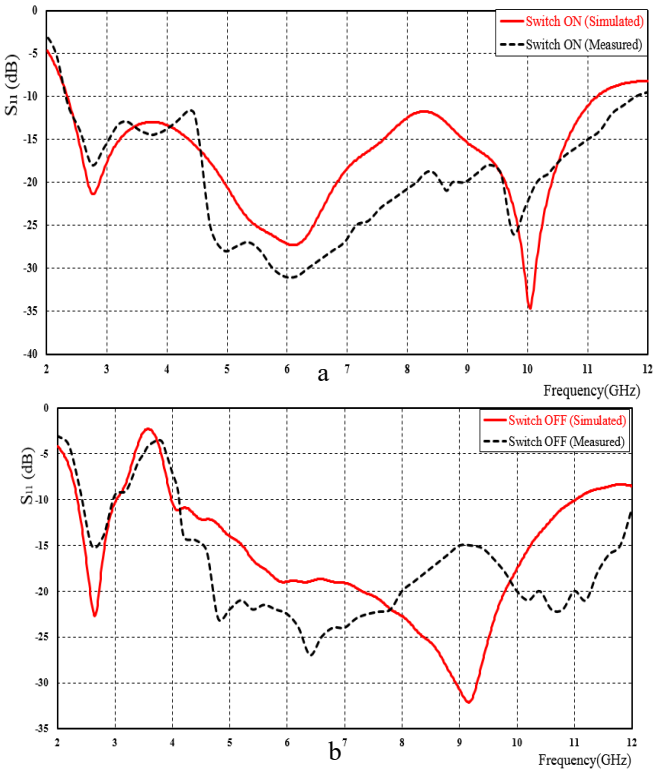

Fig. 9. (a) The simulated (solid) and measured (dashed) reflection coefficients S_{11} when switch is ON state.(b): The simulated (solid) and measured (dashed) reflection coefficients S_{11} when switch is OFF state.

The measured and simulated antenna gain values versus frequency are shown in Fig. 10. It is observed that the gain is nearly stable with small fluctuation when the switch in the ON state, so that it is suitable for sensing the UWB frequency spectrum. However, the gain drops sharply to -4 dBi within the notched band when the switch is in the OFF state. The measured gain is slightly below the simulated gain due to the space loss of the measuring environment.

The simulated and measured radiation patterns of the proposed underlay cognitive radio antenna at the frequencies 2.75 and 6.25 GHz are shown in Fig. 11. It is clear that the radiating patterns have a bidirectional pattern in the y-z plane

(E-plane) and an omnidirectional pattern at the x-z plane (H-plane) for both frequencies. Consequently, the antenna is suitable for the portable underlay cognitive radio gadgets.

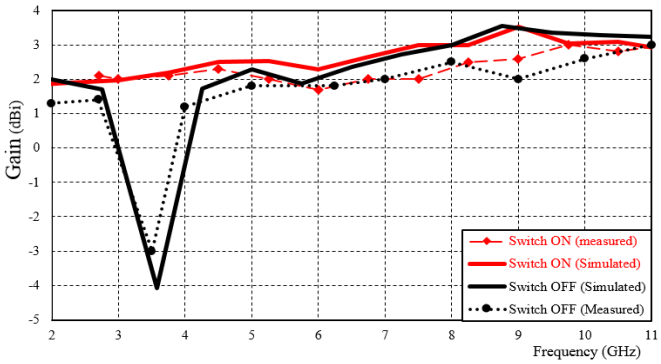

Fig. 10. The simulated (solid) and measured (dashed) gain in dBi of the proposed antenna for the two switching states

V. CONCLUSION

A printed monopole ultra-wide band (UWB) antenna with a reconfigurable band notch for underlay cognitive radio applications is designed successfully. With the aid of PIN diode and CSRR, a reconfigurable broadband notch centered at 3.5GHz and extended along the frequency range (2.9-3.9) GHz is produced. The sensing mode of the proposed antenna has a fractional bandwidth equal to 130.6% over the frequency range (2.3-11.16) GHz. The proposed antenna has an omnidirectional H-plane radiation pattern, which is suitable for portable devices. In addition, the gain value is about 2.5 dBi over the entire sensing range except for the notched band at which it drops to value less than -4 dB. Furthermore, the fabricated version of the proposed antenna gives measurements that are in good agreement with the simulated results.

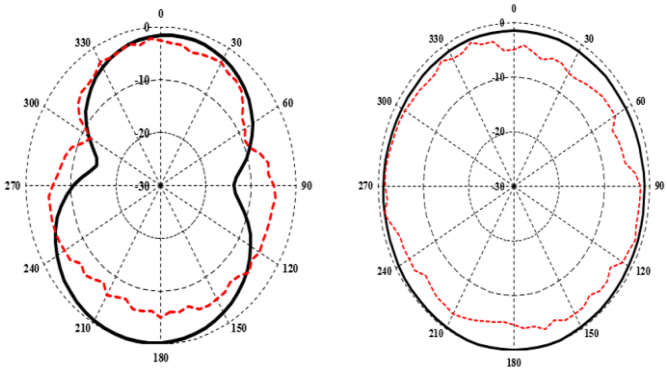

At 2.75 GHz

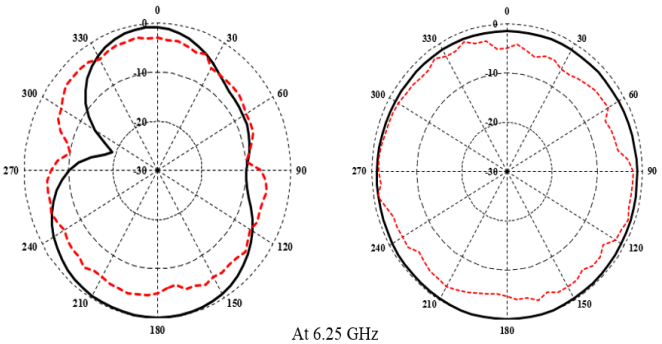

At 6.25 GHz

(a) (b)

Fig. 11. The simulated (solid) and measured (dashed) radiation pattern (a) E-plane (b) H-plane.

REFRENCES

[1]. Y. T. Christos Christodoulou, and Joseph Costantine, Antenna Design for Cognitive Radio. Artech House (July 1, 2016), 2016.

[2]. "Federal Communications Commission revision of Part 15 of the commission's rules regarding ultra-wideband transmission systems," FCC, Washington, DC, First Report and Order FCC, V48, pp. 1–118, 2002.

[3]. A. Naghar, A. V. Alejos, O. Aghzout, and M. Essaidi, "Compact microstrip omnidirectional ultrawideband antenna with dual broadband nested U-shaped slots and flat frequency response," Microwave and Optical Technology Letters, vol. 57, no. 12, pp. 2854–2856, 2015.

[4]. K. S. Ryu and A. A. Kishk, "UWB antenna with single or dual band-notches for lower WLAN band and upper WLAN band," IEEE Transaction on Antennas and Propagation, vol. 57, no. 12, pp. 3942–3950, 2009.

[5]. N. Ojaroudi, and M. Ojaroudi, "Novel Design of Dual Band-Notched Monopole Antenna With Bandwidth Enhancement for UWB Applications," IEEE Antennas and Wireless Propagation Letters, vol. 12, pp. 698–701, 2013.

[6]. A. Valizade, C. Ghobadi, J. Nourinia, N. Ojaroudi, and M. Ojaroudi, "Band-notch slot antenna with enhanced bandwidth by using Ω-shaped strips protruded inside rectangular slots for UWB applications," Applied Computational Electromagnetics Society Journal, vol. 27, no. 10, pp. 816–822, 2012.

[7]. M. Al-Husseini, A. Ramadan, A. El-Hajj, K. Y. Kabalan, Y. Tawk, and C. G. Christodoulou, "Design based on complementary split-ring resonators of an antenna with controllable band notches for UWB cognitive radio applications," 2011 IEEE International Symposium on Antennas and Propagation Society (APSURSI), pp. 1120–1122, 2011.

[8]. Y. Li, W. Li, and Q. Ye, "A reconfigurable triple-notch-band antenna integrated with defected microstrip structure band-stop filter for ultra-wideband cognitive radio applications," International Journal on Antennas and Propagation, vol. 2013, no. June, 2013.

[9]. N. Ojaroudi, N. Ghadimi, Y. Ojaroudi, and S. Ojaroudi, "A novel design of microstrip antenna with reconfigurable band rejection for cognitive radio applications," Microwave and Optical Technology Letters, vol. 56, no. 12, pp. 2998–3003, 2014.

[10]. N. Tasouji, J. Nourinia, C. Ghobadi, and F. Tofigh, "A novel printed UWB slot antenna with reconfigurable band-notch characteristics," IEEE Antennas and Wireless Propagation Letters, vol. 12, pp. 922–925, 2013.

[11]. R. Bazaz, S. K. Koul, and A. Basu, "A monopole ultra-wideband antenna with reconfigurable band-notch," 2011 IEEE Indian Antenna Week (IAW)- Workshop on Advanced Antenna Technology, 2011.

[12]. D. Draskovic, J. R. O. Fernandez, and C. Briso Rodriguez, "Planar ultrawideband antenna with photonically controlled notched bands," International Journal on Antennas and Propagation, vol. 2013, 2013.

[13]. S. Nikolaou, N. D. Kingsley, G. E. Ponchak, J. Papapolymerou, and M. M. Tentzeris, "UWB elliptical monopoles with a reconfigurable band notch using MEMS switches actuated without bias lines," IEEE Transaction on Antennas and Propagation, vol. 57, no. 8, pp. 2242–2251, 2009.

[14]. Z. N. Chen, T. S. P. See, and X. Qing, "Small ground-independent planar UWB antenna," 2006 IEEE International Symposium on Antennas and Propagation Society (APSURSI), pp. 1635–1638, 2006.

[15]. CST: "Computer Simulation Technology Based on FIT Method", 2015.

[16]. P. KAUR, R. NEHRA, and M. KADIAN, "Design of Improved Performance Rectangular Microstrip Patch Antenna Using Peacock and Star Shaped DGS," International Journal of Electronics Signals and Systems, pp. 33–37, 2013.

[17]. J. M. Noras, R. A. Abd-Alhameed, Y. I. Abdulraheem, A. S. Abdullah, H. J. Mohammed, and R. S. Ali, "Design of a uniplanar printed triple band-rejected ultra-wideband antenna using particle swarm optimisation and the firefly algorithm," IET Microwaves, Antennas and Propagation, vol. 10, no. 1, pp. 31–37, 2016.

[18]. N. X. P. Semiconductors, "Bap64-02," NXP Semicond. Malaysia Sdn. Bhd., no. May, pp. 1–9, 2015.

[19]. Y. Zhang, W. Hong, C. Yu, Z.-Q. Kuia, Y.-D. Don and J.-Y. Zhou, "Planar ultra wideband antennas with multiple notched bands based on etched slots on the patch and/or split ring resonators on the feed line," IEEE Transactions on Antennas and Propagation, vol. 56, no. 9, pp. 3063–3068, 2008.

[20]. R. Movahedinia and M. N. Azarmanesh, "Ultra-wideband band-notched printed monopole antenna," IET Microwaves, Antennas and Propagation, vol. 4, no. 12, p. 2179, 2010.

[21]. S. R. Emadian and J. Ahmadi-shokouh, "Modified Ground Circle Like-Slot Antenna with Dual Band- Notched Characteristics for Super UWB Applications," Applied Computational Electromagnetics Society Journal, vol. 30, no. 4, pp. 436–443, 2015.